Bioorganic Chemistry 52 (2014) 44–49

Contents lists available at ScienceDirect

Bioorganic Chemistry

journal homepage: www.elsevier.com/locate/bioorg

Crystal structure of phosphoramide-phosphorylated thymidylate synthase reveals pSer127, reflecting probably pHis to pSer phosphotransfer

Piotr Wilk [a,1], Adam Jarmuła [a,1], Tomasz Ruman [b,1], Katarzyna Banaszak [c], Wojciech Rypniewski [c], Joanna Cieśla [a], Anna Dowierciał [a], Wojciech Rode [a,*]

[a] Nencki Institute of Experimental Biology, Polish Academy of Sciences, Warszawa, Poland
[b] Rzeszów University of Technology, Faculty of Chemistry, Bioorganic Chemistry Laboratory, 6 Powstańców Warszawy Ave., 35-959 Rzeszów, Poland
[c] Institute of Bioorganic Chemistry, Polish Academy of Sciences, Poznań, Poland

ARTICLE INFO

Article history:
Received 11 September 2013
Available online 21 November 2013

Keywords:
Thymidylate synthase
Phosphorylation
Potassium phosphoramidate
Crystal structure
Phosphotransfer

ABSTRACT

Crystal structure is presented of the binary complex between potassium phosphoramidate-phosphorylated recombinant *C. elegans* thymidylate synthase and dUMP. On each monomer a single phosphoserine residue (Ser127) was identified, instead of expected phosphohistidine. As ^{31}P NMR studies of both the phosphorylated protein and of potassium phosphoramidate potential to phosphorylate different amino acids point to histidine as the only possible site of the modification, thermodynamically favored intermolecular phosphotransfer from histidine to serine is suggested.

1. Introduction

Thymidylate synthase (TS; EC 2.1.1.45), a target in chemotherapy [1], catalyzes the $N^{5,10}$-methylenetetrahydrofolate (meTHF)-dependent C(5)-methylation of dUMP [2], required for DNA synthesis. Potential non-catalytic activities, including an oncogene-like activity [3], suggest the enzyme protein to be a potential translational regulator of cellular gene expression [4].

Possible phosphorylation of mammalian TS was first shown by incubation of rat hepatoma cells with ^{32}P and demonstration of the enzyme in the cells to undergo labelling [5]. Later the modification was suggested to be a potential cause of differing enzyme properties, including sensitivity to inactivation by FdUMP and some analogues, of TSs from parental and FdUrd-resistant mouse leukemia L1210 cells [6]. Furthermore, different recombinant TSs have been found to be phosphorylated *in vitro* by CK2, with the human enzyme the modification concerning Ser124 and causing inactivation [7,8]. Of considerable interest was an observation that recombinant TS protein expressed in bacterial cells may undergo phosphorylation on histidine residue(s), lowering the enzyme catalytic activity [9].

To learn more about molecular aspects of TS phosphorylation on histidine residue(s), studies were undertaken on chemical phosphorylation by potassium phosphoramidate (KPA), believed unable to modify hydroxyaminoacids [10], and crystallization of *C. elegans* recombinant enzyme protein. Unexpectedly, the solved structure of the phosphorylated enzyme-dUMP binary complex (*Ce*pTS-dUMP) showed a phosphoserine, instead of phosphohistidine residue, therefore KPA potential to phosphorylate different residues was further tested.

2. Materials and methods

2.1. Materials

Potassium phosphoramidate (KPA) was prepared as previously described [11]. Pro-Q® Diamond Phosphoprotein Gel Stain and SYPRO® Ruby Protein Gel Stain were from Molecular Probes. Amino acids were purchased from Sigma–Aldrich (Poland) and were of 98+% purity.

Abbreviations: TS, thymidylate synthase; KPA, potassium phosphoramidate; MOAC, metal oxide/hydroxide affinity chromatography; *Ce*TS, recombinant *C. elegans* TS; MOAC-separated, from its phosphorylated fraction; *Ce***p**TS, *Ce*TS phosphorylated by KPA and phosphoprotein-enriched by MOAC; **p**His, phosphohistidine; **p**Ser, phosphoserine; DTT, 1,3-dithiothreitol.

* Corresponding author. Address: Nencki Institute of Experimental Biology, 3 Pasteur Street, 02-093 Warszawa, Poland.
E-mail address: rode@nencki.gov.pl (W. Rode).

[1] These authors contributed equally to this work.

0045-2068/$ - see front matter © 2013 Elsevier Inc. All rights reserved.
http://dx.doi.org/10.1016/j.bioorg.2013.11.003

2.2. TS preparation

C. elegans [12] coding region was cloned into pPIGDM4+stop vector and expressed in a TS-deficient TX61$^-$ (a kind gift from Dr. W. S. Dallas) *E. coli* strain. The enzyme was purified as previously described [13]. Phosphatase inhibitors (50 mM NaF, 5 mM Na-pyrophosphate, 0.2 mM EGTA, 0.2 mM EDTA and 2 mM Na_3VO_4; following the ammonium sulfate precipitation step, NaF and Na-pyrophosphate concentrations were decreased to 10 mM and 2 mM, respectively) were present in all purification buffers. TS activity was monitored, and kinetic parameters of the enzyme-catalyzed reaction determined, as previously described [14]. The final enzyme preparation was separated into phosphorylated and non-phosphorylated fractions according to Wolschin et al. [15], using metal oxide/hydroxide affinity chromatography (MOAC) on $Al(OH)_3$ beads. The non-phosphorylated fraction, referred to as *Ce*TS, was used in further studies.

2.3. Analysis in TS preparations of protein pattern and phosphorylation

Phosphoprotein/protein detection was performed on polyacrylamide gels, using the Multiplexed Proteomics® Phosphoprotein Gel Stain Kit according to the manufacturer's protocol. Phosphorylated protein species, stained with ProQ-Diamond, were visualized on a 300 nm UV transilluminator and the image recorded using the 590 ± 40 nm filter. The same gel was subsequently stained with SYPRO Ruby Protein Gel Stain, the protein again visualized on a 300 nm UV transilluminator, and the image recorded using the 590 ± 40 nm filter. PeppermintStick™ phosphoprotein molecular mass standards, containing phosphorylated (ovalbumin, 45 kDa; β-casein, 23.6 kDa) and non-phosphorylated (β-galactosidase, 116.25 kDa; bovine serum albumin, 66.2 kDa; avidin, 18 kDa) proteins, provided controls (both positive and negative).

2.4. Protein phosphorylation with KPA

The protein (2–60 mg) was incubated in 50 mM Tris–HCl or phosphate buffer pH 7.5, in the presence of 12–16% KPA, for 24 h at 25–27 °C. A constant decrease of enzyme activity was observed during the course of the reaction, whereas no loss of activity was noted in controls containing KCl at a concentration equal to that of KPA. The reaction product was enriched with the use of a metal oxide affinity chromatography (MOAC) method (*cf.* 2.2), yielding 10% of protein phosphorylated to an extent similar to that observed with the phosphorylated fraction of recombinant TS protein, referred to as *Ce***p**TS.

2.5. NMR analyses

All NMR spectra were obtained with BrukerAvanceII spectrometer operating in quadrature mode at 500.13 MHz for ^{1}H and 202.46 MHz for ^{31}P nuclei. The residual peaks of deuterated solvents were used as internal standards in ^{1}H NMR method. The internal standard used in ^{31}*P NMR* was inorganic phosphate (P_i), having its resonance at 2.15 ppm (at pH 7.8), 2.05 ppm (pH 7.5), 1.65 ppm (at pH 5.0) and 0.0 ppm (at pH 1.5). All samples were analyzed using gradient-enhanced ^{1}H-^{31}P Heteronuclear Multiple Bond Correlation (HMBC) experiments. The HMBC experiments were optimized for long range couplings by using different $^3J_{P-H}$ values (1–20 Hz). The ^{1}H NMR spectra were obtained with and without the use of HDO suppression method. All buffer solutions used for NMR spectroscopy were based on deuterium oxide of ~100%D purity (Armar Chemicals AG).

2.6. NMR-controlled amino acid (His, Arg, Lys, Cys, Tyr, Ser) phosphorylation procedure

2.6.1 Deuterated water solution of amino acid (10 mg of amino acid in 200 μL of D_2O) was shaken with KPA (at the amino acid:KPA molar ratio of 1:10). The reaction mixture was shaken for 24 h at 318 K temperature and afterwards the NMR sample was prepared by addition of 350 μL of deuterium oxide and 200 μL of deuterium oxide-based Tris–HCl buffer solution (pH 7.8).

2.6.2 Phosphorylation reaction was performed as shown above (in 2.6.1) but for the applied amino acid:KPA molar ratio of 1:3.

2.6.3 Phosphorylation was performed as in 2.6.1 but for the applied amino acid:KPA molar ratio of 1:5. Besides, the reaction was run not only at pH 7.8, but also at pH 5, 9.5 and 11.

2.7. Crystallization and data collection

The protein was dialyzed against 5 mM Tris HCl buffer, pH 7.5, containing 5 mM DTT and concentrated using an Amicon Centricon centrifugal filter (*cf.* Ref. [16]). Crystals were grown by the vapor diffusion method in hanging drops at 4 °C. A 2.5 μL sample of the protein solution (14.5 mg/ml) in 5 mM Tris–HCl buffer pH 7.5, containing 5 mM DTT and 8 mM dUMP, was mixed with an equal volume of well solution, containing 0.1 M Bis-Tris buffer pH 6.5, 0.2 M $(NH4)_2SO_4$ and 25% PEG 3350, the final solution mixed and allowed to equilibrate with 0.5 mL of the well solution.

X-ray diffraction data were collected from a single flash-frozen crystal at the BESSY Synchrotron using an X-ray wavelength of 0.918 Å.

2.8. Data processing: structure determination and refinement

Data were processed with the use of DENZO and SCALEPACK [17]. The structure was determined by molecular replacement carried out with Phaser from the CCP4 package [18], using the *Ce*TS-dUMP complex structure (PBD ID: 4IRR) as the search model. The correctness of the structure was evaluated using Sfcheck and Procheck from the CCP4 suite. Some X-ray data and model refinement parameters are presented in Table 1.

3. Results and discussion

3.1. Crystallization approaches

Initial attempts to obtain crystals of phosphorylated *C. elegans* TS protein, involving KPA treatment of previously obtained protein

Table 1
Data collection and refinement statistics summary for reported TS complex.

Crystal and refinement parameters	*C. elegans* TS(KPA)-P-dUMP
PDB ID	4ISW
Lattice type	Trigonal
Space group	P 3_2 2 1
Unit cell parameters	a = 133.44 Å; c = 153.97 Å
Wavelength (Å)	0.918
Resolution range (Å)	38.5–3.14 (3.19–3.14)[a]
No. of unique reflections	27855 (1206)
Completeness	99.1 (87.8)
Redundancy	12.6 (6.2)
$<I/\sigma(I)$	6.9 (2.15)
No. of reflections used in refinement	26459
*R*factor (%)	23.4
R_{free} factor (%)	26.9
RMS bond (Å)	0.0052
RMS angle (°)	1.0337

[a] Values in parentheses are for highest-resolution shell.

crystals and crystallization in the presence of KPA (*cf.* Ref. [19]), did not result in diffracting crystals. Therefore in further experiments the enzyme was treated with KPA in solution and the phosphorylated protein crystallized following phosphoprotein enrichment by the affinity chromatography on $Al(OH)_3$ (Fig. 1). The latter yielded a series of crystals showing rather poor diffraction properties. The diffraction data, collected for the best-diffracting crystal, representing the *Ce***p**TS-dUMP complex, structure, were processed to a resolution of 3.14 Å.

3.2. Structure of phosphorylated CeTS complex with dUMP

The final *Ce***p**TS-dUMP model, consisting of a single dimer in the asymmetric unit, has been deposited in PDB as 4ISW (Fig. 2 and Table 1). Each subunit in the model includes amino acids 23–312 and a single molecule of dUMP. The Vm coefficient of 5.9 $Å^3$/Da indicates a large solvent content of 79%, a value very similar to that of 78% in the crystal of the *Ce*TS-dUMP complex formed by the non-phosphorylated enzyme protein.

In the course of refinement, particular attention was paid to local environments of the side chains of histidines, yet no electron densities were found that would be larger than those of water molecules. Surprisingly, the 2Fo-Fc map indicated strong electron densities (of about 6σ) located around Ser127 in both subunits of the enzyme dimer (not shown). While those electron densities were too large to represent molecules of water, their size corresponded well with phosphate groups of phosphoserines or ordered sulfate anions. Although the model resolution was not sufficient to distinguish reliably between the two possibilities, several premises pointed to phosphate groups on Ser127 as the true chemical identities behind those electron densities: (i) the analysis of the high-resolution structure of ligand-free *Ce*TS, obtained in the presence of ammonium sulfate, indicated the occurrence of sulfate anions only in the active site of the enzyme, and not in the proximity of

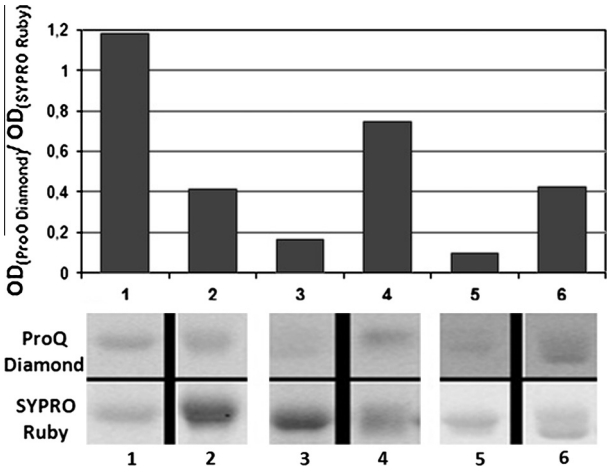

Fig. 1. Phosphorylation of commercially available phosphoalbumin (**1**) and TS protein (**2–6**), analyzed following SDS/polyacrylamide gel electrophoresis: Gels, containing phosphorylated ovalbumin (**1**; positive control) or recombinant *C. elegans* TS preparations, including phosphoprotein-enriched following KPA treatment of *Ce*TS (*Ce***p**TS; *cf.* 2.4), used for crystallization (**2**), non-phosphorylated enzyme protein (*Ce*TS; *cf.* 2.2), separated from the phosphorylated form based on being not bound by MOAC; this preparation was treated with KPA and MOAC-enriched to obtain *Ce***p**TS (**3**), phosphorylated while expressed in *E. coli* cells, phosphoprotein-enriched (by separation from *Ce*TS; *cf.* 2.2) by MOAC (**4**), dissolved crystals of the non-phosphorylated TS-dUMP complex (**5**) and dissolved crystals of the *Ce***p**TS-dUMP complex (**6**), were treated first with the Pro-Q® Diamond Phosphoprotein Gel Stain, to detect phosphorylated protein (middle panel) and then with the SYPRO Ruby Protein Gel Stain, to detect total protein (bottom panel). The protein phosphorylation level (middle panel band) related to protein level (the corresponding bottom panel band) is presented in the upper panel.

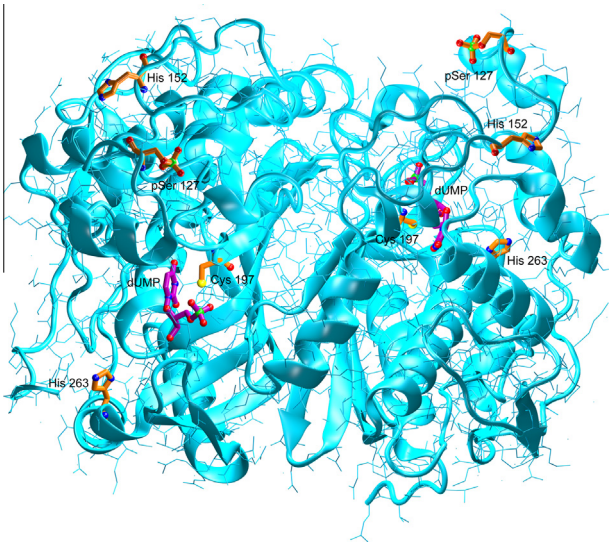

Fig. 2. Crystal structure of the dimeric *Ce***p**TS-dUMP complex. dUMP, catalytic Cys197, His152, His263 and **p**Ser127 are shown as licorice and labelled. Carbon atoms are orange or violet (dUMP), and oxygen, nitrogen, phosphorus and sulfur atoms are red, blue, green and yellow, respectively. This figure was prepared with VMD [27] and rendered with Raster3D [28].

Ser127, (ii) after several cycles of refinement with Refmac5, the position of the sulfate anion in the structure of the *Ce***p**TS-dUMP complex was unfavorable due to a close distance of ~2.5 Å between one of the oxygen atoms of the potential sulfate anion and the C_β atom of Ser127, (iii) the phosphate anion, modeled as attached to Ser127 (i.e., as a part of the resulting phosphoserine), was placed in a more ordered manner, compared to the sulfate anion (modeled adjacent, but unattached to Ser127), reflected by the temperature factor of the phosphate moiety of phosphoserine **p**Ser127 (84 $Å^2$) smaller than that of the sulfate anion (91 $Å^2$); moreover, the B factor of **p**Ser phosphate moiety was closer to a value of B factor for aminoacidic part of **p**Ser (66 $Å^2$), than was sulfate ion *vs.* unmodified serine (58 $Å^2$), (iv) the analysis of dissolved pTS crystals showed the protein to be still phosphorylated, thus excluding potential dephosphorylation in the process of crystallization. Thus, an apparent phosphorylation target was the Ser127 residue, instead of an expected histidine.

3.3. Phosphorylation site in KPA-phosphorylated CeTS in view of ^{31}P NMR spectra

The ^{31}P NMR spectrum of phosphorylated *C. elegans* thymidylate synthase contained the resonance at 2.3 ppm, belonging to inorganic phosphate, and three *upfield* shifted peaks of a visible singlet-multiplicity in the *ca.* −7 to −10 ppm region. The assignment of the singlet resonances, based on those previously described [20], strongly suggested the peaks in the negative spectrum region to reflect N-phosphorylated histidine species. Moreover, analyses of time-dependent changes of the ^{31}P NMR spectrum following acidification (after 1 h at pH 3) confirmed the presence of phosphorus in a phosphoramidate (acid-labile) bond (Fig. 3, insert). Of note is that at pH 7.5 there were no visible peaks in the spectrum that might suggest the presence of phosphate moiety attached covalently to other amino-acids (Fig. 3), even following a 2–4 week period of storage of such samples in a refrigerator. Interestingly, the results remained the same when in one sample pH was lowered to 5.0 and it was stored for three weeks (not shown).

In order to assess a possibility of the presence in the sample of another phospho-amino acid, escaping detection, a simple calculation of peak area and intensity may be applied. With the inorganic

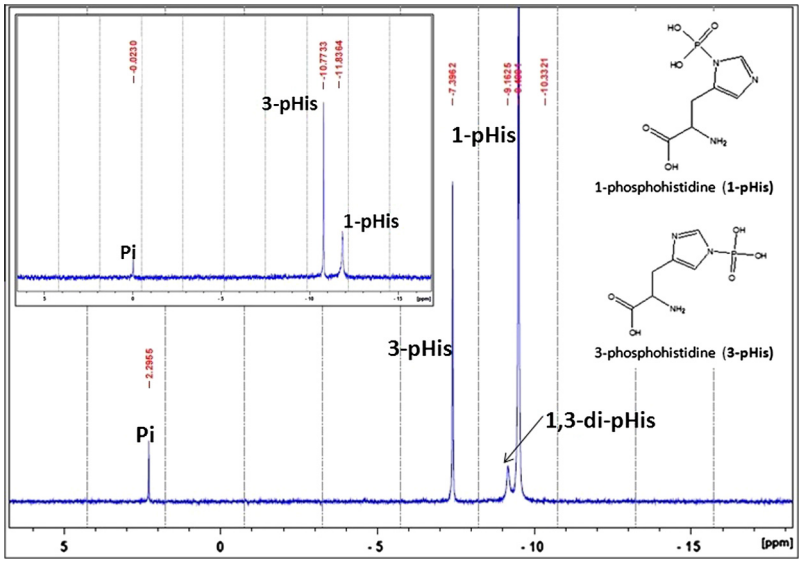

Fig. 3. ^{31}P NMR spectrum of the recombinant *C. elegans* TS preparation prepared for crystallization by phosphoprotein-enrichment by MOAC following phosphoramidate treatment, measured at pH 7.5 (*Ce***p**TS). Typically, 0.5 ml of the protein sample, containing 200 mM Tris–HCl pH 7.5, 20% sucrose and 10 mM mercaptoethanol, was mixed with 0,2 ml D2O (99,8%D). The resonances correspond to inorganic phosphate (Pi) at -2.30 ppm, 3-phosphohistidine (3-**p**His) at −7.40 ppm, 1-phosphohistidine (1-**p**His) at −9.50 ppm and 1,3-diphosphohistidine (1,2-di-**p**His) at -9.16 ppm. The insert presents the corresponding spectrum measured after 1 h incubation of the sample at pH 3.

phosphate resonance area considered 1.0, the total area of phosphohistidine species amounted to 34.6. Assuming that all of the enzyme histidine side-chains were monophosphorylated, the resonance area, resulting from the presence of another singly phosphorylated amino acid (for example serine), should be not less than 3.8 (34.63/9 histidine residues). Moreover, the fewer phosphorylated histidine residues in the protein, the higher the area of singly-phosphorylated species. Assuming the area of the inorganic phosphate resonance 1.0, it is almost impossible that a phosphoserine resonance of dd or tr-multiplicity, found always in the 6 to −1 ppm range, would be non-visible. Moreover, the signal-to-noise ratios of **p**His resonances were in the 25 to 460 range, further supporting the above conclusion.

3.4. Testing KPA capacity to phosphorylate different amino acids

The amino acids selected to be used as substrates in the phosphorylation experiments belong to three groups, differing by containing nitrogen (His, Arg, Lys), oxygen (Ser, Tyr) or sulfur (Cys) heteroatoms in the side chain. Other amino acids were not considered due to (i) containing a non-reactive aliphatic, aromatic or amide side chain (Gly, Ala, Val, Leu, Ile, Pro, Phe, Gln, Asn), (ii) lacking a relatively acidic hydrogen atom at a heteroatom present in the side chain (Met, Trp), (iii) having an acidic side chain that may undergo phosphorylation to a very unstable products (Asp, Glu) or (iv) being represented in the group of the selected substrates by another amino acid of a similar structure (Thr similar to Ser). The ^{31}P NMR method was chosen for analysis of the post-reaction mixtures.

The ^{31}P NMR chemical shifts of the phosphorylated amino acid resonances were in agreement with those previously presented [20]. The phosphorylation reaction run under mild conditions (318 K, pH between 5 and 11, the amino acid:KPA molar ratios ranging from 1:3 to 1:10) led to a rather fast phosphorylation of histidine, yielding its 1- and 3-phosphates, along with the 1,3-diphosphate form. The latter was true for each pH point tested (5, 7.5, 9.5 and 11) and no significant α-NH_2 phosphorylation product was observed. Arginine was phosphorylated mainly on α-NH_2 group, with only traces of other products (with phosphorylated guanidine nitrogen) found at pH ⩾ 9.5. Unlike arginine, the lysine side chain nitrogen was found to undergo phosphorylation under rather basic conditions (pH ⩾ 5). Moreover, not only the terminal NH_2 but also α-NH_2 group was phosphorylated, although to much lower extent. With lysine, as with histidine, the higher was pH of the reaction mixture, the higher the yield of new phosphoramide species, presumably due to a rising concentration of the neutral –NH_2 form in solution. Cysteine underwent *S*-phosphorylation with much lower yield, compared to the side-chain amino group *N*-phosphorylation, with the *S*-phosphate product found in all samples at pH 5, 9.5 and 11. Of particular interest is that *O*-phosphorylation of the serine side-chain was found to take place only at pH ⩾ 9.5, and with a very low yield. As with basic amino acids, the higher the pH, the higher was concentration of phosphorylated serine. No evidence of *O*-phosphorylation of serine was found at the pH range of 5–8 (*cf.* Ref. [21]).

Of particular interest was testing KPA reactivity towards serine. The reaction was run at pH 5, 9.5 and 11, using only a 5-fold excess of KPA over the amino acid, to prevent the KPA and/or inorganic phosphate (Pi) resonances to interfere with a relatively small phospho-amino acid resonance. The reaction was slowed down by addition of 0.35 ml of deuterium oxide and 0.2 ml of 0.1 M Tris–HCl buffer (pH 7.8). Following the reaction at pH 5, ^{31}P NMR analysis showed no phospho-serine (PSer) resonances. Triplet-like PSer resonances, at 6.60 and 6.79 ppm, became apparent following the reaction at pH 9.5 and 11, respectively. With the hydrogen decoupling applied, the ^{31}P NMR spectrum showed a singlet resonance, indicating the triplet (or double doublet) resonance pattern to result from the P–H coupling. Of note is that while the ^{31}P spectrum collected following the reaction at pH 9.5 included three resonances, assigned to Pi, PSer and KPA, their areas amounting to 47.7%, 3.8% and 48.5% of the total peak area, respectively, at pH 11 the corresponding values were 20.2%, 10.8% and 68.9%, respectively. Thus the higher pH value, the more PSer is formed, presumably due to a higher participation of the form with deprotonated hydroxyl group of serine side chain.

3.5. Hypothetical explanation of Ser127 modification

In view of the above presented results, while serine residue phosphorylation by KPA appears highly improbable, phosphate

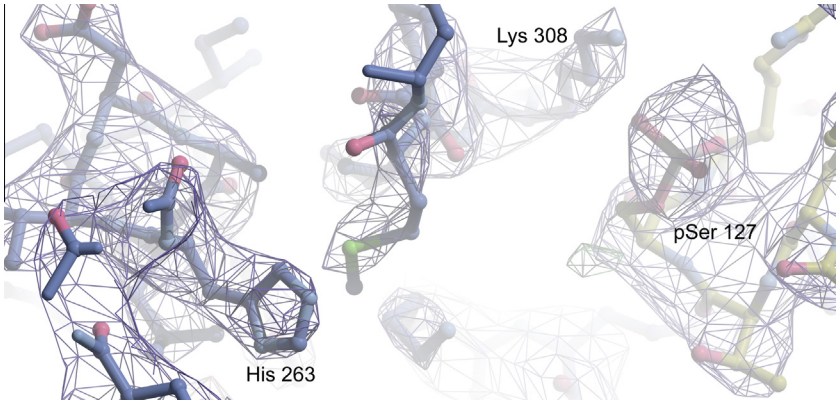

Fig. 4. 2Fo-Fc **e**lectron density map at 2σ showing **p**Ser127 from subunit A and Lys 308 and His263 from the neighboring TS molecule. This figure was prepared with Coot [29] and rendered with Raster3D.

group identity of the electron density observed in the vicinity of Ser127 in each subunit of the *Ce***p**TS-dUMP complex seems highly probable. Looking for a solution of the latter paradox, a hypothesis may be put forward that what is found in the crystal structure, is an effect of the transfer of the phosphate moiety from a histidine residue to Ser127 in the course of crystallization of the highly concentrated enzyme protein in a weakly acidic solution (pH in the range of 5.5–6.5). In this context, it is important to note that N-phosphoamino acids, including phosphohistidine, phosphoarginine and phospholysine, are known to be labile under acidic conditions, as opposed to O-phosphoamino acids, including phosphoserine, phosphothreonine and phosphotyrosine that remain stable under such conditions [22]. Moreover, **p**His has a higher ΔG of hydrolysis (−12 to −13 kcal/mol) compared to O-phosphoamino acids (−6.5 to −9.5 kcal/mol) [23], making the transfer of the phosphoryl group from **p**His to surrounding target molecules even more plausible. However, it should be considered whether the phosphoryl transfer might not be promoted by the buffer used for the protein crystallization, containing 2.5 mM DTT, highly nucleophilic and being a good leaving group. Although TS preparation studied did not contain DTT, the structure and chemical reactivity of the latter is very similar to mercaptoethanol that was present in TS preparation (at 10 mM concentration) and NMR samples (at ∼6 mM concentration) of phoshorylated TS (*cf.* Fig. 3). Mercaptoethanol contains also both thiol and hydroxyl groups and shows not only polarity very similar to that of DTT, but also strong nucleophilic properties. In fact, DTT could be considered a dimeric derivative of mercaptoethanol. Also the pKa value of the mercaptoethanol thiol is 9.6, hence similar to the corresponding values of 9.2 and 10.1, characteristic for the two DTT thiol groups. It appears therefore that DTT was not responsible for the observed phosphate transfer.

Of note is that a similar possibility of false localization of the modification has been observed in the MS studies applying collisional activation in analysis of arginine-phosphorylated peptides resulting from enzymatic phosphorylation, the results pointing to a partial rearrangement of phosphorylation from arginine onto serine and glutamic acid residues [24]. Another example involved inter- or intra-molecular phosphate transfer from histidine to aspartate within a synthetic nonapeptide analyzed by nano-ultra-performance liquid chromatography-nano-electrospray ionization-tandem MS. Moreover, similar phosphotransfer has been observed to take place during sample storage [25].

Considering the above presented transfer hypothesis, a potential source of the phosphate group should be sought. One possibility would be a phosphohistidine residue on another thymidylate synthase molecule and intermolecular phosphotransfer. Recently Dar and Chakraborti [26] presented evidence of intermolecular phosphotransfer from His to Ser, being important for catalytic activity of nucleoside diphosphate kinase. In the *Ce***p**TS-dUMP crystal structure, Ser127 of the subunit A is 11.5 Å away from the closest His263 (the distance between Ser127 γO and His263 εN was measured) on another TS molecule (Fig. 4). A small rearrangement of mutual positions of two neighboring TS molecules could arguably lessen the distance, boosting the chances for a direct transfer. An alternative, involving an intra-molecular phosphotransfer, seems less plausible, as the closest His152 is located approximately 13 Å away from Ser127 (the distance between Ser127 γO and His152 εN was measured), the latter being an excessively long distance for a direct transfer. Considering whether any of the two His residues, His152 and His263, was phosphorylated following KPA treatment, results of initial NanoLC-MS/MS studies of a TS preparation identical with that used in crystallization revealed two singly phosphorylated peptides, ^{148}YVDC**H**TDYSGQGVDQLAEVIR^{168} and ^{242}VCGLKPGTLV**H**TLGDA**H**VYSN**H**VDALK^{268}. While further CID fragmentation allowed to localize phosphorylation at His152 in the former peptide, it indicated only a certain probability of phosphorylation of His263 in the latter (P. Wilk, P. Palmowski, A. Rogowska-Wrzesinska, unpublished).

3.6. Comparison of Ce**p**TS-dUMP and CeTS-dUMP models

In the *Ce***p**TS-dUMP structure, in each of the two subunits, A and B, the phosphate group of **p**Ser127 is linked by hydrogen bond to either Lys308 from the neighboring thymidylate synthase molecule (subunit A) or Gly 124 of the same subunit (subunit B). The superimposition of the structures of the *Ce***p**TS-dUMP and *Ce*TS-dUMP complexes did not reveal any significant conformational differences between the models. Small differences observed for the side chains of some amino acids can be explained either due to a large conformational freedom of those amino acids (located usually at the protein surface) or due to different accuracies of both models, owing to their different resolutions. It should be noted, though, that actual effects of modification of a protein could manifest themselves in a more transparent way through an altered dynamics of this protein, rather than through its single static structure. Such a "dynamic format" of influence has been observed in the case of human TS phosphorylated on Ser124 [8].

Acknowledgments

This work was supported by the National Science Centre (Grant No. 2011/01/B/NZ6/01781) and the Ministry of Science and Higher Education (Grant No. N301 3948 33). Authors are grateful to the core facilities of the International Institute of Molecular and Cell

Biology in Warsaw, Poland, for access to the X-ray generator and to Dr. Roman Szczepanowski for support during data collection.

References

[1] N.L. Lehman, Expert Opin. Investig. Drugs 11 (2002) 1775–1787.
[2] C.W. Carreras, D.V. Santi, Annu. Rev. Biochem. 64 (1995) 721–762.
[3] L. Rahman, D. Voeller, M. Rahman, S. Lipkowitz, C. Allegra, J.C. Barrett, F.J. Kaye, M. Zajac-Kaye, Cancer Cell 5 (2004) 341–351.
[4] J. Liu, J.C. Schmitz, X. Lin, N. Tai, W. Yan, M. Farrell, M. Bailly, T. Chen, E. Chu, Biochim. Biophys. Acta 1587 (2002) 174–182.
[5] W.A. Samsonoff, J. Reston, M. McKee, B. O'Connor, J. Galivan, G.F. Maley, F. Maley, J. Biol. Chem. 272 (1997) 13281–13285.
[6] J. Cieśla, T. Frączyk, Z. Zieliński, J. Sikora, W. Rode, Acta Biochim. Pol. 53 (2006) 189–198.
[7] T. Frączyk, K. Kubiński, M. Masłyk, J. Cieśla, U. Hellman, D. Shugar, W. Rode, Bioorg. Chem. 38 (2010) 124–131.
[8] A. Jarmuła, T. Frączyk, P. Cieplak, W. Rode, Bioorg. Med. Chem. 18 (2010) 3361–3370.
[9] T. Frączyk, T. Ruman, D. Rut, E. Dąbrowska-Maś, J. Cieśla, Z. Zieliński, K. Sieczka, J. Dębski, B. Gołos, P. Wińska, E. Wałajtys-Rode, D. Shugar, W. Rode, Pteridines 20 Special Issue (2009) 137–142.
[10] Y.F. Wei, H.R. Matthews, Methods Enzymol. 200 (1991) 388–414.
[11] M.C. Pirrung, K.D. James, V.S. Rana, J. Org. Chem. 65 (2000) 8448–8453.
[12] P. Wińska, B. Gołos, J. Cieśla, Z. Zieliński, T. Frączyk, E. Wałajtys-Rode, W. Rode, Parasitology 131 (2005) 247–254.
[13] J. Cieśla, K.X. Weiner, R.S. Weiner, J.T. Reston, G.F. Maley, F. Maley, Biochim. Biophys. Acta 1261 (1995) 233–242.
[14] W. Rode, T. Kulikowski, B. Kędzierska, D. Shugar, Biochem. Pharmacol. 36 (1987) 203–210.
[15] F. Wolschin, S. Wienkoop, W. Weckwerth, Proteomics 5 (2005) 4389–4397.
[16] A. Dowiercial, P. Wilk, W. Rypniewski, T. Frączyk, A. Jarmuła, K. Banaszak, M. Dąbrowska, J. Cieśla, W. Rode, Pteridines 24 (2013) 87–91.
[17] Z. Otwinowski, W. Minor, Methods Enzymol. 276 part A (1997) 307–326.
[18] Computational Project, Number 4. The CCP4 suite: programs for protein crystallography, Acta Cryst. D 50 (1994) 760–763.
[19] S. Morera, M. Chiadmi, G. LeBras, I. Lascu, J. Janin, Biochemistry 34 (1995) 11062–11070.
[20] T. Ruman, K. Długopolska, A. Jurkiewicz, D. Rut, T. Frączyk, J. Cieśla, A. Leś, Z. Szewczuk, W. Rode, Bioorg. Chem. 38 (2010) 74–80.
[21] K. Kowalewska, P. Stefanowicz, T. Ruman, T. Frączyk, W. Rode, Z. Szewczuk, Biosci. Rep. 30 (2010) 433–443.
[22] S. Klumpp, J. Krieglstein, Eur. J. Biochem. 269 (2002) 1067–1071.
[23] J.M. Kee, T.W. Muir, ACS Chem. Biol. 7 (2012) 44–51.
[24] A. Schmidt, G. Ammerer, K. Mechtler, Proteomics 13 (2013) 945–954.
[25] M.-B. Gonzalez-Sanchez, F. Lanucara, M. Helm, C.E. Eyers, Biochem. Soc. Trans. 41 (2013) 1089–1095.
[26] H.H. Dar, P.K. Chakraborti, Biochem. J. 430 (2010) 539–549.
[27] W. Humphrey, A. Dalke, K. Schulten, J. Mol. Graph. 14 (1996) 33–38.
[28] E.A. Merritt, D.J. Bacon, Meth. Enzymol. 277 (1997) 505–524.
[29] P. Emsley, B. Lohkamp, W.G. Scott, K. Cowtan, Acta Crystallogr. D 66 (2010) 486–501.